Réf I. 12

Waves in Random Media 3 (1993) 71–83. Printed in the UK

Intensity fluctuations of spherical acoustic waves propagating through thermal turbulence*

Ph Blanc-Benon and D Juvé

Laboratoire de Mécanique des Fluides et d'Acoustique, URA CNRS 263, Ecole Centrale de Lyon BP 163, 69131 Ecully Cedex, France

Received 27 October 1992

Abstract. The intensity fluctuations of acoustic waves that propagate through thermal turbulence are investigated under well controlled laboratory conditions. Two heated grids in air are placed horizontally in a large anechoic room and the mixing of the free convection plumes above them generates a homogeneous isotropic random thermal field. The spectrum of refractive index fluctuations is accurately described by a modified von Karman model which takes into account the entire spectrum of turbulence. Experimental data are obtained by varying both the frequency of the spherical wave and the distance of propagation. In this paper we concentrate on the variance of the normalized intensity fluctuations and on their probability distributions. These measurements cover all the regimes from weak scattering to strong scattering including the peak of the intensity variance. Experimental values of the scintillation index are compared with classical theoretical predictions and also with the results of recent numerical simulations. The classical probability density functions (log-normal, exponential, I–K) are tested against the measured probability distributions. The generalized gamma distribution, which varies smoothly from log-normal to exponential as a function of two parameters, appears to represent the experimental data for a very large range of scattering conditions.

1. Introduction

Acoustic waves traversing a turbulent medium develop random changes in phase and amplitude. Measurements of the intensity fluctuations in the atmosphere or ocean have been obtained by several authors [1, 2]. However, the uncertainties with regard to relevant environmental parameters, namely the velocity and temperature variations, make it difficult to assess their individual influences on acoustic scintillation. The propagation of sound waves through turbulent velocity fields has already been investigated under laboratory conditions [3–5]. For temperature fields experiments usually employed a water tank in which the random temperature field was produced by a heater array mounted at the bottom [6]. In this arrangement discrete impurities appear, such as minute air bubbles due to thermal degassing, and present an additional and poorly controlled parameter [7]. An installation with a grid in air eliminates this problem and has been choosen in this work. To simulate atmospheric or oceanic conditions of acoustic propagation, it is assumed that the acoustic wavelength λ remains small compared with the integral length scale L_T of the temperature field, which, in turn, is smaller than the range of z propagation, i.e. $z \gg L_T \gg \lambda$.

In our previous work [8–10], investigations of spatial correlation functions and mean intensity repartitions demonstrated the importance of correct modelling of the turbulent

* Presented at the International Scintillation Meeting, Seattle, Washington, August 1992.

0959-7171/93/020071+13$07.50

thermal field using a modified von Karman spectrum, and the role of the particular form of the incident wave (spherical or extended sources). Good agreement was obtained between the experimental data and the theoretical estimates deduced from the parabolic approximation of the stochastic Helmholtz equation.

In this paper we present experimental results for the variance of the normalized intensity fluctuations (or scintillation index) and for the probability density functions. These measurements cover the whole regime from weak to strong scattering. These are compared with theoretical or numerical predictions given in the literature [11–18].

2. Experimental arrangement

The two heated grids as well as the locations of the acoustic transmitter and receivers are shown in figure 1. The grids consist of a plane arrangement of conductors with a square mesh M of 9 cm and a maximum heating power of 32 kW. They are placed horizontally in a large anechoic room (10 m × 7 m × 8 m) and the mixing of the free convection plumes above them generates the thermal turbulent field. The second grid can either be placed adjacent to the first one to increase the distance of propagation up to 4.4 m, or shifted above the first grid to change the size M of the heating cells from 9 to 4.5 cm. The acoustic propagation measurements were made at the height $H = 180$ cm corresponding to 20 or 40 times the mesh size M.

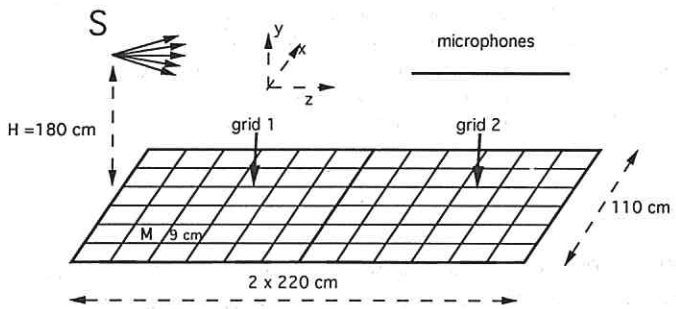

Figure 1. Experimental set-up.

With the two adjacent grids ($M = 9$ cm), the mean temperature rise above ambient was 27 °C and the relative temperature $T'/\langle T\rangle$ had a RMS value of 0.017. The statistical uniformity of the thermal field was achieved within 0.5 °C excluding 1.5 meshes near the edges. The one-dimensional spectrum $F_{T'}(K_1)$ was measured with a fast Fourier transform analyser (Nicolet 660 A) in the range 0.5–200 Hz with a constant bandwith of 0.5 Hz. Frequencies were converted into wavenumbers K_1 by a Taylor hypothesis based on the mean upward velocity (1.25 m s^{-1} measured with a hot wire). Results are given in figure 2 and compared with the one-dimensional spectrum $F_{T'}(K_1)$ deduced from the modified von Karman spectrum $\Phi_f(K)$, where $K = \| \boldsymbol{K} \|$, by

$$F_{T'}(K_1) = \int_{K_1}^{\infty} K\Phi_f(K)\,\mathrm{d}K \tag{1}$$

$$\Phi_f(K) = 0.033C_f^2(K^2 + 1/L_0^2)^{-11/6}\exp(-K^2/K_m^2) \tag{2}$$

$$C_f^2 = 1.91(\sqrt{\langle T'^2\rangle}/2\langle T\rangle)^2 L_0^{-2/3} \qquad K_m = 5.91/l_0. \tag{3}$$

The outer scale of turbulence L_0 is related to the integral scale of turbulence L_T ($L_0 = 1.339\ L_T$). The integral scale L_T deduced by integration of the spatial correlation curve is 7.6 cm. The inner scale l_0 is related to the high-frequency cut-off of the spectrum and was estimated to be 0.1 cm. The index changes that may be induced by the velocity fluctuations in the z direction prove to be negligible; indeed an upper limit is given by u'_y/c (u'_y being the fluctuating component of the velocity in the upward direction) and measurements indicate that $u'_y/c = 6 \times 10^{-4}$. The same measurements were also made with the two shifted grids ($M = 4.5$ cm). The mean temperature rise was 35 °C and the RMS value of $T'/\langle T\rangle$ reached 0.025. The mean velocity in the upward direction was 1.5 m s^{-1} with a fluctuating component u'_y of 0.25 m s^{-1}. The integral scale L_T is 5 cm. Additional details are given in Blanc-Benon [10].

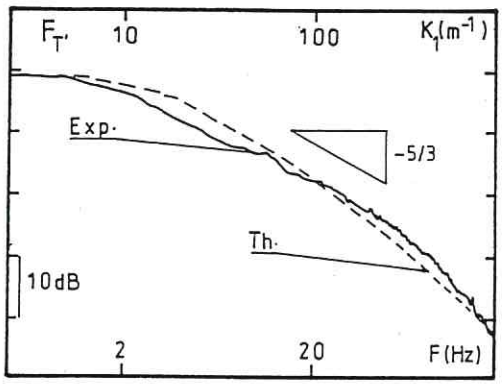

Figure 2. Comparison between the experimental one-dimensional spectrum of temperature fluctuations $F'_T(K_1)$ and the theoretical spectrum deduced from the von Karman expression $\Phi_f(K)$.

The spherical acoustic waves were generated by small piezoelectric ultrasonic sources ($\nu = 23.5, 31, 39, 75$ kHz). The transducers consist of a one-piece housing with a circular diaphragm of diameter $2a = \frac{1}{2}$ in for the highest frequency and $2a = 1$ in for the other ones ($5 \leqslant ka \leqslant 9$). The directivity pattern of these piston-like sources exhibits a large main lobe (total angle of 30° to 60° at −3 dB). For our measurements of intensity fluctuations near the axis of the transducers the point-source model can then be used safely. The transmitted signals were received on $\frac{1}{4}$ in microphones (Bruël & Kjaer 4135) located along the z axis. The acoustic intensity and the higher moments were obtained by a digital treatment of the acoustic pressure signal. In a first step the pressure signal is heterodyned to a frequency of 5 kHz. Then using a digital acquisition (Difa TS 9000, an 8-channel system with 12 bit of resolution and 8 × 64 K word memory) interfaced with a HP 9000/330 workstation, the pressure field is sampled with a period of 20 μs and the data are stored on the disc system for later postprocessing. Typically we then calculate the different moments of the intensity $\langle (I - \langle I\rangle)^n\rangle$ using 50 blocks of 65 536 samples corresponding to an averaging time of 65.5 s ($\langle\rangle$ indicates an ensemble average and n is the order of the moment). The probability density functions of the normalized intensity $I/\langle I\rangle$ are evaluated using 128 classes.

In figure 3 we have plotted our experimental conditions using the Φ–Λ diagram devised by Flatté [11]. In this scheme acoustic conditions can be categorized into 'saturated',

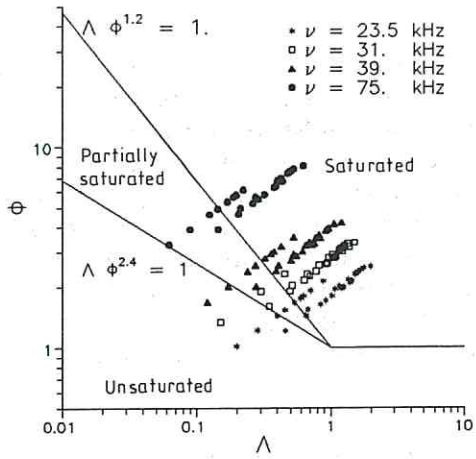

Figure 3. Experimental conditions in a Φ–Λ diagram. Zone boundaries are calculated for a Kolmogorov spectrum $\Phi_f(K) = 0.033\ C_f^2 K^{-11/3}$.

'partially saturated' and 'unsaturated' zones based on the RMS value expected for the phase variance $\Phi = \sqrt{2L_T k^2 z \langle \mu^2 \rangle}$, ($\mu = -T'/2\langle T \rangle$; k, acoustic wavenumber; z, distance of propagation), and on the diffraction parameter $\Lambda = z/kL_T^2$. The boundaries between the different regions are evaluated for a Kolmogorov spectrum of the index fluctuation $\Phi_f(K) = 0.033 C_f^2 K^{-11/3}$ (K, turbulent wavenumber).

Typical evolutions of normalized intensity fluctuations $I/\langle I \rangle$ versus time are visualized on figures 4–7 for different scatterring conditions obtained by varying the distance of propagation, the frequency of the source and the characteristics of the thermal turbulent field. The recording time of each plot is 1.31 s corresponding to a block of 65 536 samples. In each figure we indicate the value of the parameters Φ–Λ, the experimental normalized variance σ^2 and the theoretical value σ_B of the Born solution (equation (5)). In the region of unsaturated fluctuations, $\Lambda\Phi^{2.4} < 1$, the presence of the coherent field is clear together with a small amount of intensity fluctuations (for example $\nu = 23.5$ kHz; $z = 0.5$ m on figures 4(a) and 5(a)). In the saturation region $\Lambda\Phi^{1.2} > 1$, the records exhibit narrow high peaks and the coherent field disappears.

3. Normalized variance of intensity

In figure 8 we compare our measurements of the normalized variance of the intensity fluctuations σ^2 with known theoretical or numerical predictions. As usual, all the curves are plotted using the variance of the log-amplitude fluctuations σ_χ^2 evaluated by Rytov's method with the assumption of a pure Kolmogorov spectrum $\Phi_f(K) = 0.033 C_f^2 K^{-11/3}$. In this approach, the scintillation index of a spherical wave is expressed in the following form [12, 13]:

$$\sigma^2 = \exp(0.41\sigma_B^2) - 1 \tag{4}$$

with

$$\sigma_B^2 = 4\sigma_\chi^2 = 1.23 C_f^2 k^{7/6} z^{11/6}. \tag{5}$$

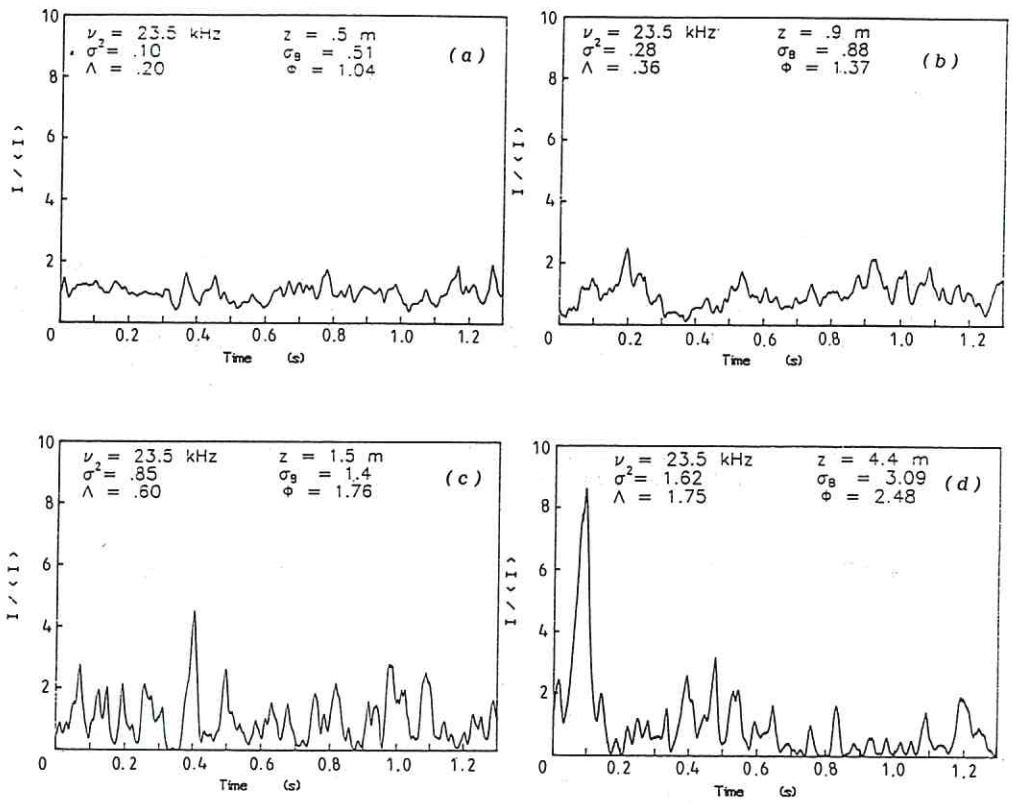

Figure 4. Typical evolution of the intensity fluctuations versus time for different distances of propagation. The integral scale L_T is 7.6 cm and the RMS value of $T'/\langle T\rangle$ is 0.017.

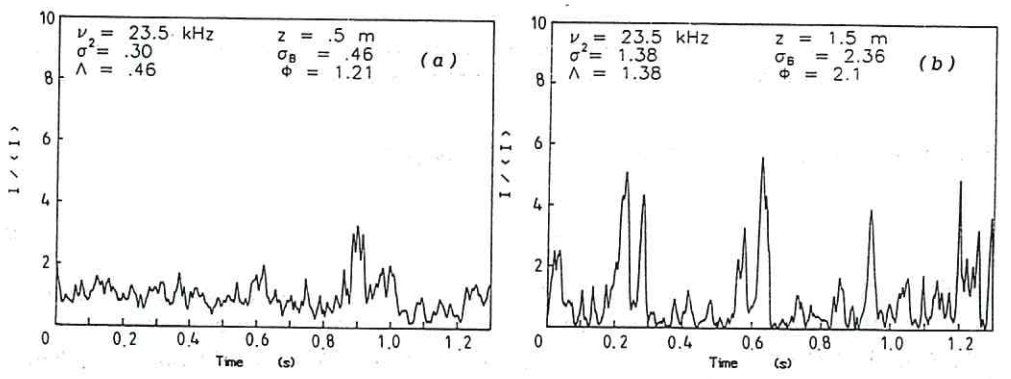

Figure 5. Typical evolution of the intensity fluctuations versus time for different distances of propagation. The integral scale L_T is 5 cm and the RMS value of $T'/\langle T\rangle$ is 0.025.

We note that Rytov's solution (curve 1) is valid for short pathlengths and/or weak turbulence conditions for which $\sigma^2 < 0.2$. For increasing values of σ_B the scintillation index σ^2 reaches a maximum value greater than unity and then slowly decreases when σ_B increases further. In strong turbulence the experimental behaviour of σ^2 corresponds to the

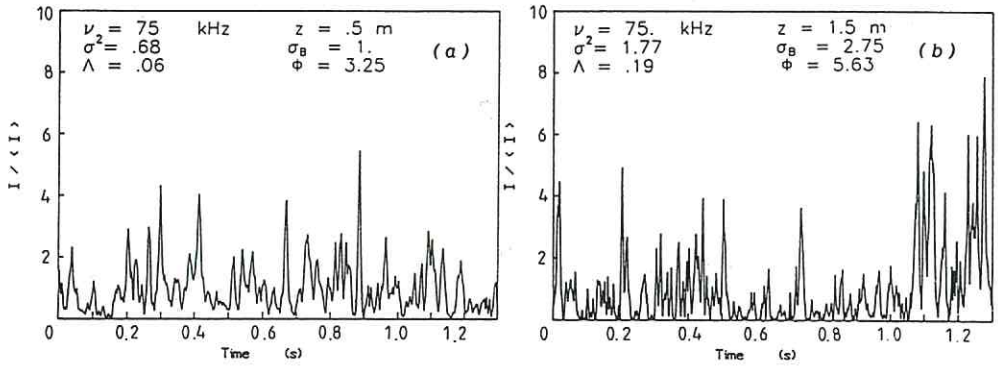

Figure 6. Typical evolution of the intensity fluctuations versus time for different distances of propagation. The integral scale L_T is 7.6 cm and the RMS value of $T'/\langle T\rangle$ is 0.017.

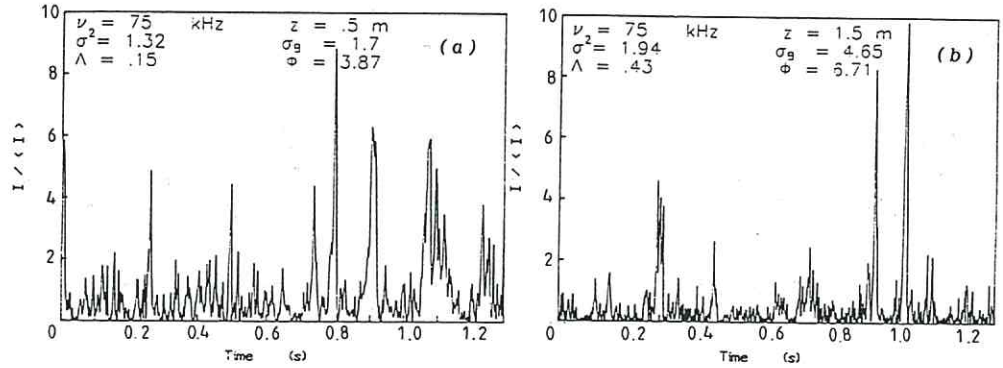

Figure 7. Typical evolution of the intensity fluctuations versus time for different distances of propagation. The integral scale L_T is 5 cm and the RMS value of $T'/\langle T\rangle$ is 0.025.

prediction of the asymptotic theory of Prokhorov *et al* [15] (curve 2):

$$\sigma^2 = 1 + 2.8\sigma_B^{-4/5} \qquad (\sigma_B^2 \gg 1). \tag{6}$$

Between these two well defined regimes of propagation we observe a large spreading of the measurements. For a fixed value of σ_B obtained for various combinations of the frequency ν, the distance z and the statistical characteristics of the thermal turbulence, the temporal evolutions of the acoustic intensity are very different (compare, for example, figures 4(b) and 6(a) where the values of σ_B are very close), and the corresponding levels of the variance σ^2 are in the ratio of 1 to 2, which is much greater than the measurement error. This plot clearly indicates that the evolution of the scintillation index σ^2 cannot be described with only one parameter. This is in agreement with previous theoretical descriptions of the second-order moment of the intensity which use a two-parameter solution depending on the diffraction and the scattering strength [11, 14, 24].

In addition to Rytov's solution ($\sigma_B \ll 1$) and the asymptotic theories ($\sigma_B \gg 1$), many models have been proposed to describe the intensity fluctuations and to extend the domain

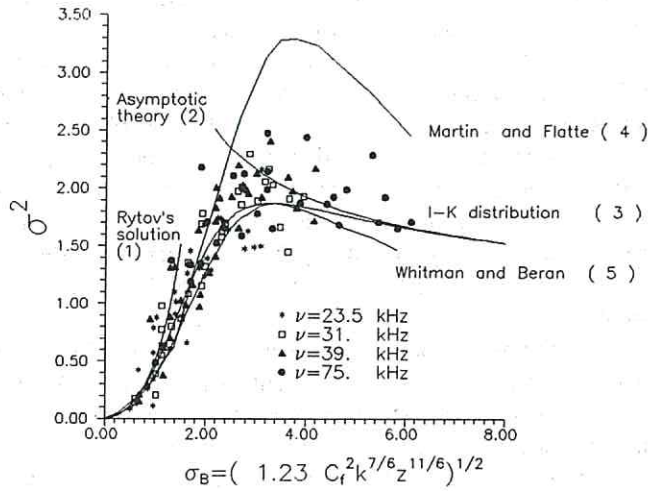

Figure 8. Variation of the normalized variance of intensity σ^2 with σ_B (equation (5)). Comparison with theoretical estimates of equations (4), (6) and (7) and numerical simulations of [17, 18].

of validity of the predictions to the intermediary scattering conditions. Some authors have developed mathematical analysis for the probability density function of the intensity, and recently the I–K distributions received a great attention [16]; others have solved the fourth-order moment equation using numerical simulations [17] or multi-scale developments [18].

The variance of the intensity estimated with an I–K distribution is displayed on curve 3 of figure 8. For this phenomenological model [16, 25] σ^2 is a function of two variables α and ρ and takes the form

$$\sigma^2 = \frac{2}{(1+\rho)^2}\left(\frac{1}{2} + \frac{1+\rho}{\alpha}\right). \tag{7}$$

Andrews *et al* ([16]) have obtained expressions for the parameters α and ρ in terms of the physical characteristics of the turbulence by using results from perturbation techniques for weak turbulence and the asymptotic theory for strong turbulence. In the case of a zero inner scale of turbulence l_0, the parameters α and ρ are defined as

$$\alpha = 0.71\sigma_B^{4/5} \tag{8}$$

and

$$\rho = \frac{4.88}{\alpha\sigma_B^2(1+0.2\sigma_B^2)}. \tag{9}$$

The variance σ_B^2 is defined by equation (5) and calculated with the experimental values of ν, z and C_f^2. For weak scattering and for strong scattering our experimental data are in a reasonable agreement with their predictions. However, for the intermediate regime, where the effect of the frequency of the source is important, the experimental data and the theoretical results differ by a factor larger than 1.5.

Finally, in figure 8, we plot the point-source intensity variances obtained by Martin and Flatté [17] with a 3D numerical simulation and by Whitman and Beran [18] with a two-scale asymptotic solution. The difference between these two theoretical methods is very large (see curves 4 and 5). Our measurements of σ^2 as a function of σ_B differ significantly from the theoretical estimates as soon as σ_B exceeds the value of 2. We note that most of our experimental values lie between the predicted curves 4 and 5. Up to this point our comparisons have been based on the assumption of a zero inner scale. However, a finite inner scale can lead to a larger value for the scintillation index in the region of the peak value; then we have estimated this effect by evaluating the parameter β/R_f defined as the ratio between the inner scale and the size of the first Fresnel zone [17], $\beta/R_f = 0.338 l_0/\sqrt{z/k}$. The maximum value of β/R_f, 0.025, is obtained with a frequency of 75 kHz and a distance of propagation of 0.5 m, for all the other experimental conditions β/R_f never exceeds a value of 0.015. In [17] it is shown that a significant increase of σ^2 is obtained only for $\beta/R_f > 0.1$. So in our experimental conditions this inner scale effect cannot explain the difference between our data and previous numerical simulations.

The effect of the outer scale of turbulence has also to be explored to explain the difference between our experimental data and the predictions of Martin and Flatté ([17] curve 4). Indeed it is known that a decrease in L_0 induces a reduction of the maximum of the scintillation index. The numerical simulations of Martin and Flatté [28], for plane waves, indicate that at a fixed value of σ_B the peak of σ^2 is reduced by a factor of 1.7 when L_0 is of the same order of magnitude than R_f. In our experiments the ratio L_0/R_f varies from 1 to 6, and our data for the scintillation index are smaller than the predicted ones by a factor of 1.5 to 2. However, it is difficult to draw a definitive conclusion as for the influence of L_0 because, according to our knowledge, no similar numerical simulations exist for a spherical wave propagating in a 3D medium modelled by a von Karman spectrum. In addition it is not convenient to point out a clear experimental effect of the outer scale L_0 because the integral scale is limited to a variation from 5 to 7.6 cm, and because any change of L_0 affects other turbulent parameters (turbulence intensity, inner scale).

4. Probability density functions

Figures 9–12 provide experimental histograms of the normalized intensity fluctuations $W(I/\langle I\rangle)$ measured for various conditions: two frequencies ($\nu = 23.5, 75$ kHz), four distances of propagation ($z = 0.5, 0.9, 1.5, 4.4$ m) and two integral length scales ($L_T = 7.6, 5$ cm). Each one of these probability density functions corresponds to one of the temporal evolution of the normalized intensity $I/\langle I\rangle$ reported previously (figures 4–7). In figure 9 we clearly visualize the modification of the probability density functions (PDF) obtained by increasing the distance of propagation from $z = 0.5$ to 4.4 m and keeping constant the frequency of the source ν and the integral scale of turbulence L_T. This corresponds to a continuous variation from weak scattering to strong scattering. Similar trends are observed when we are varying either L_T (figure 10) or ν (figures 11 and 12).

For weak fluctuations the application of the central limit theorem leads to a log-normal distribution for the intensity I [12]:

$$W(I) = \frac{1}{\sqrt{2\pi} I \sigma} \exp\left[-\left(\ln\left(\frac{I}{\langle I\rangle}\right) + \frac{\sigma^2}{2}\right)^2 \frac{1}{2\sigma^2}\right] \tag{10}$$

where the variance σ^2 and the mean intensity $\langle I\rangle$ are evaluated from the experimental data. For extremely strong fluctuations, the Rayleigh distribution in amplitude or the negative

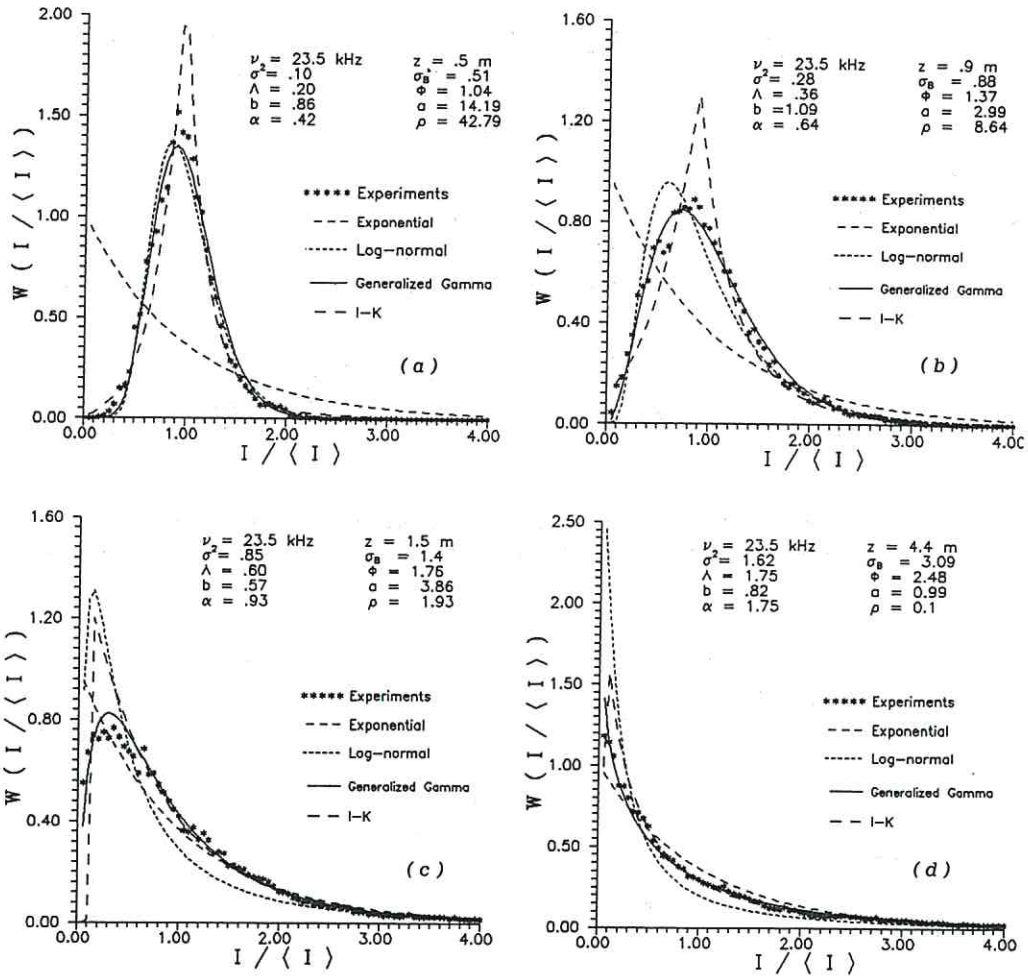

Figure 9. Evolution of the probability distribution of the normalized intensity for different distances of propagation. The integral scale L_T is 7.6 cm and the RMS value of $T'/\langle T\rangle$ is 0.017.

exponential distribution in intensity is generally accepted (Strohbehn *et al* [19]):

$$W(I) = \frac{1}{\langle I\rangle}\exp\left(-\frac{1}{\langle I\rangle}\right). \tag{11}$$

However, there is no theoretical prediction of the PDF valid for all propagation conditions and especially for the intermediate region. Over the years, many attempts [20–23] have been made to suggest general PDFs based on at least two parameters. In our experiment the relevance of two of them to describe wave propagation in turbulent media has been tested for a large range of scattering conditions.

First we have considered the I–K distribution introduced by Andrews *et al* [16]. The PDF of the normalized intensity $u = I/\langle I\rangle$ is given by

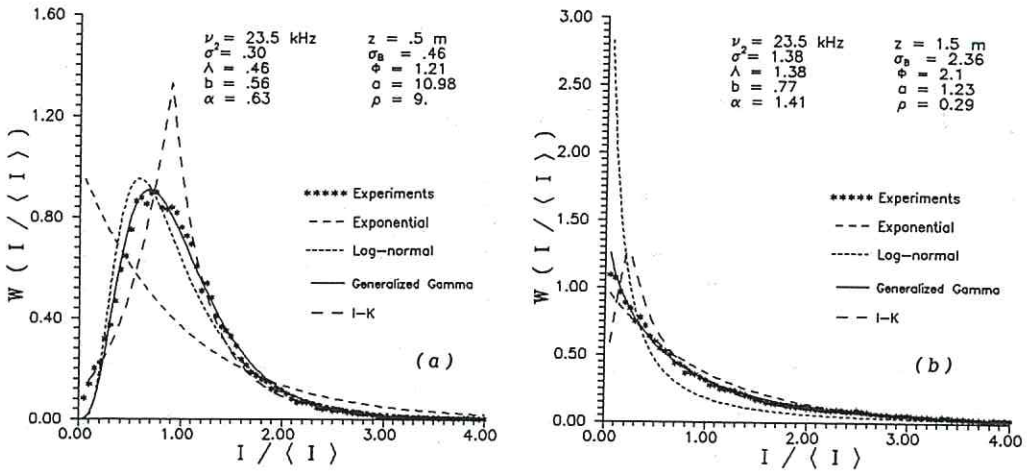

Figure 10. Evolution of the probability distribution of the normalized intensity for different distances of propagation. The integral scale L_T is 5 cm and the RMS value of $T'/\langle T\rangle$ is 0.025.

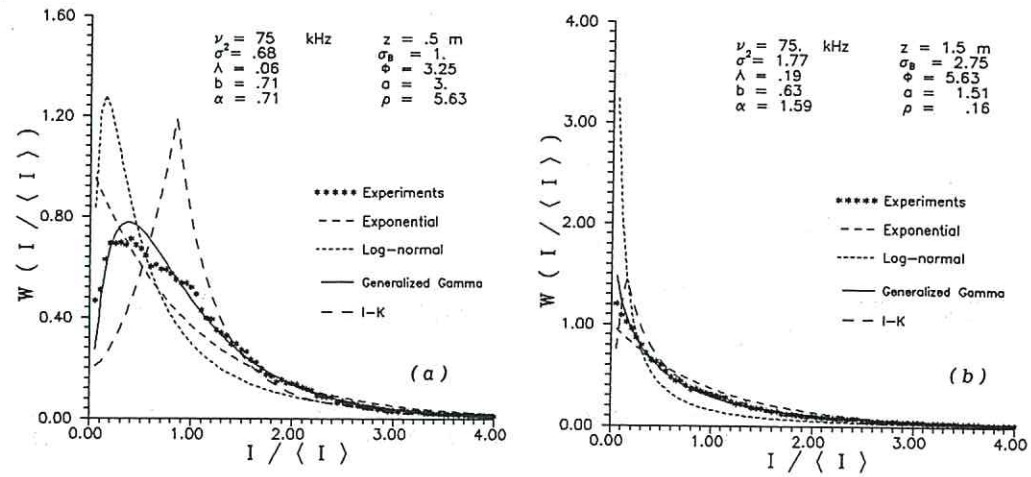

Figure 11. Evolution of the probability distribution of the normalized intensity for different distances of propagation. The integral scale L_T is 7.6 cm and the RMS value of $T'/\langle T\rangle$ is 0.017.

$$W(u) = \begin{cases} 2\alpha(1+\rho)\left[\dfrac{1+\rho}{\rho}u\right]^{(\alpha-1)/2} K_{\alpha-1}(2\sqrt{\alpha\rho})I_{\alpha-1}(2\sqrt{\alpha(1+\rho)u}) & \text{if } u < \rho/1+\rho \\ 2\alpha(1+\rho)\left[\dfrac{1+\rho}{\rho}u\right]^{(\alpha-1)/2} K_{\alpha-1}(2\sqrt{\alpha(1+\rho)u})I_{\alpha-1}(2\sqrt{\alpha\rho}) & \text{if } u > \rho/1+\rho \end{cases} \tag{12}$$

where K_α and I_α are the modified Bessel functions. The two parameters α and ρ are related to physical parameters of the turbulence (equations (8) and (9)). So, by measuring the characteristics of the turbulence as we have done in our experiments, it is possible to predict the shape of the PDF and all the higher-order statistical moments.

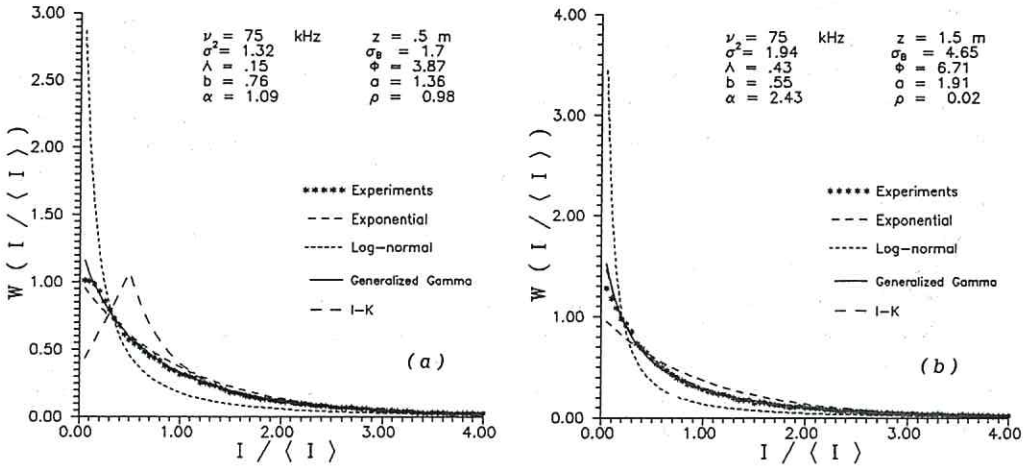

Figure 12. Evolution of the probability distribution of the normalized intensity for different distances of propagation. The integral scale L_T is 5 cm and the RMS value of $T'/\langle T\rangle$ is 0.025.

The second distribution we tested is the generalized gamma distribution that varies smoothly from log-normal to exponential as a function of two parameters a and b (Blanc-Benon [5], Blanc-Benon and Juvé [9], Blanc-Benon [10], Ewart and Percival [23] and Ewart [24]). This PDF takes the form

$$W(I) = bd^{a}/\Gamma(a)I^{ab-1}\exp(-dI^{b}) \tag{13}$$

$$d = (\Gamma(a+1/b)/\Gamma(a))^{1/b} \tag{14}$$

where Γ is the gamma function. The parameters a and b are deduced from the measurements of the moments m_2 and m_3 by solving the following two non linear equations

$$m_2 = \frac{\langle I^2\rangle}{\langle I\rangle^2} = \frac{\Gamma(a)\Gamma(a+2/b)}{\Gamma^2(a+1/b)} \tag{15}$$

$$m_3 = \frac{\langle I^3\rangle}{\langle I\rangle^3} = \frac{\Gamma^2(a)\Gamma(a+3/b)}{\Gamma^3(a+1/b)}. \tag{16}$$

These estimated PDFs (equations (10)–(13)) are plotted on figures 9–12. For each histogram we indicate the values of the generalized gamma parameters (a, b) and of the I–K parameters (α, ρ) deduced from the measurements. As is expected, for extremely weak turbulence ($\sigma^2 < 0.2$) the intensity fluctuations are log-normally distributed and for strong turbulence our data tend towards the exponential distribution.

The comparison of the experimental PDF with the I–K distribution is not successful. The I–K PDF is a sharply peaked function with a cusp at the maximum which is not observed in the data. We note that for all our experiments the I–K distribution greatly overestimated the maximum of the PDF. This discrepancy has already been observed by Churnside and Frehlich [25] for optical scintillation in the atmosphere.

In addition, as we have already noticed for the time evolution of the acoustic intensity, the PDFs obtained for a same value of the variance σ_B^2 and various values of ν, L_T or z

can be very different. In figures 9(*b*) and 11(*a*) we observed that the generalized gamma distribution takes these important variations into account very well, and, on the other hand, that the I–K PDF seems non-sensitive to these effects. In our comparison with the heuristic generalized gamma distribution, the excellent fit obtained for a wide range of scattering conditions, confirms the assertion that this PDF can be used in the modelling of the probability distribution of the intensity. Similar results have been obtained with a piston-like source (Blanc-Benon [10]).

In recent numerical simulation we have introduced a new approach to study the propagation of acoustic waves through thermal turbulence [26, 27]. The turbulent field is modelled by an ensemble of realizations generated by a superposition of one hundred or so random Fourier modes. Then through each realization the acoustic waves are propagated using a wide-angle parabolic approximation. Our first results obtained for a 2D case reinforce the opinion that the generalized gamma distribution is an appropriate law to model the intensity fluctuations from weak to strong scattering.

5. Conclusion

The intensity fluctuations of spherical acoustic waves propagating through thermal turbulence have been investigated under well controlled laboratory conditions involving heated air grids. We have presented results for the variance and the probability distributions of the normalized intensity fluctuations. These measurements cover all the regimes from weak to strong scattering.

The measurements of the scintillation index were compared with different theoretical models. In the extremely weak scattering conditions our data are in good agreement with Rytov's solution. For increasing scattering strength the experimental data reported in this paper reveal significant differences with several theories available in the literature, and we point out that the inner scale effect is not enough to explain the disparity.

For the probability distribution of the intensity it has been shown that the log-normal distribution can only be applied in the region of very small intensity fluctuations. Also the exponential intensity distribution should be restricted to very strong scattering. For the in-between conditions, the two parameter I–K distribution does not accurately describe the acoustic intensity fluctuations. Finally, the heuristic generalized gamma distribution that varies smoothly from log-normal to negative exponential as a function of two parameters, constitutes a good model to fit the experimental data for a very large range of scattering conditions.

Acknowledgment

This research was partially supported by the French Ministry of Defence (DGA-DRET).

References

[1] Daigle G A, Piercy J E and Embleton T F W 1983 *J. Acoust. Soc. Am.* **74** 1505–13
[2] Ewart T E, Macaskill C and Uscinski B J 1983 *J. Acoust. Soc. Am.* **74** 1484–99
[3] Ho C M and Kovasnay L S G 1976 *J. Acoust. Soc. Am.* **60** 40–5
[4] Candel S M, Julienne A and Juliand M 1976 Shielding and scattering by a jet flow *3rd AIAA Aero-Acoustics Conf. (Palo-Alto)* AIAA Paper 76-545

[5] Blanc-Benon Ph 1981 Effet d'une turbulence cinématique sur la propagation des ondes acoustiques *Thèse Doct. Ing.* ECL81-02 (Ecole centrale de Lyon)
[6] Stone R G and Mintzer D 1962 *J. Acoust. Soc. Am.* **34** 647–53
[7] Neubert J A and Lumley J L 1976 *J. Acoust. Soc. Am.* **64** 1148–58
[8] Blanc-Benon Ph, Chaize S and Juvé D 1986 Coherent aspects of acoustic wave transmission through a medium with temperature fluctuations *Aero Hydro Acoustics, IUTAM Symp.* ed G Comte-Bellot and J E Ffowcs-Williams (Berlin: Springer) pp 217–26
[9] Blanc-Benon Ph and Juvé D 1987 Statistical properties of acoustic waves propagating through turbulent thermal fields *11th AIAA Aero-Acoustics Conf. (Palo-Alto, CA)* AIAA paper 87-2727
[10] Blanc-Benon Ph 1987 Caractéristiques statistiques des ondes acoustiques après traversée d'une turbulence thermique *Thèse DSc* Lyon University I 87-49
[11] Flatté S M, Dashen R, Munk W H and Watson K M 1979 *Sound Transmission through a Fluctuating Ocean* (Cambridge: Cambridge University Press)
[12] Tatarski V I 1971 *The Effects of the Turbulent Atmosphere on Wave Propagation* (Jerusalem: IPST Keter)
[13] Ishimaru A 1978 *Wave Propagation and Scattering in Random Media* vol 2 (New York: Academic)
[14] Uscinski B J 1977 *The Elements of Wave Propagation in Random Media* (New York: McGraw-Hill)
[15] Prokhorov A M, Bunkin F V, Gochelasvily K S and Shishov V I 1975 *Proc. IEEE* **63** 790–811
[16] Andrews L C, Philipps R L and Shivamoggi B K 1988 *Appl. Opt.* **27** 2150–6
[17] Martin J M and Flatté S M 1990 *J. Opt. Soc. Am.* A **7** 833–47
[18] Whitman A M and Beran M J 1985 *J. Opt. Soc. Am.* A **2** 2133–43
[19] Strohbehn J W, Wang T and Speck J P 1975 *Radio Sci.* **10** 59–70
[20] Dashen R 1975 *J. Math. Phys.* **20** 894–920
[21] Parry G 1981 *Opt. Acta* **28** 715–28
[22] Uscinski B J, Macaskill C and Ewart T E 1983 *J. Acoust. Soc. Am.* **74** 1474–83
[23] Ewart T E and Percival D B 1986 *J. Acoust. Soc. Am.* **80** 1745–53
[24] Ewart T E 1989 *J. Acoust. Soc. Am.* **86** 1490–8
[25] Churnside J H and Frehlich R G 1989 *J. Opt. Soc. Am.* A **6** 1760–6
[26] Hugon-Jeannin Y 1992 Simulation numerique de la propagation d'ondes acoustiques en milieu turbulent *Thèse de Doctorat* ECL92-37
[27] Blanc-Benon Ph, Juvé D and Hugon-Jeannin Y 1992 Propagation of acoustics waves through thermal turbulence: a numerical study of intensity fluctuations *European Conf. on Underwater Acoustics* ed M Weydert (Amsterdam: Elsevier Applied Science) pp 584–7
[28] Martin J M and Flatté S M 1988 *Appl. Opt.* **27** 2111–26